5366 *Biochemistry* **2010,** *49,* 5366–5376
DOI: 10.1021/bi100523c

BIOCHEMISTRY
including biophysical chemistry & molecular biology
Article

Biophysical Investigation of the Mode of Inhibition of Tetramic Acids, the Allosteric Inhibitors of Undecaprenyl Pyrophosphate Synthase

Lac V. Lee, Brian Granda, Karl Dean, Jianshi Tao, Eugene Liu, Rui Zhang, Stefan Peukert, Sompong Wattanasin, Xiaoling Xie, Neil S. Ryder, Ruben Tommasi, and Gejing Deng*

Infectious Diseases, Novartis Institutes for BioMedical Research, Inc., Cambridge, Massachusetts 02139

Received April 7, 2010; Revised Manuscript Received May 14, 2010

ABSTRACT: Undecaprenyl pyrophosphate synthase (UPPS) catalyzes the consecutive condensation of eight molecules of isopentenyl pyrophosphate (IPP) with farnesyl pyrophosphate (FPP) to generate the C_{55} undecaprenyl pyrophosphate (UPP). It has been demonstrated that tetramic acids (TAs) are selective and potent inhibitors of UPPS, but the mode of inhibition was unclear. In this work, we used a fluorescent FPP probe to study possible TA binding at the FPP binding site. A photosensitive TA analogue was designed and synthesized for the study of the site of interaction of TA with UPPS using photo-cross-linking and mass spectrometry. The interaction of substrates with UPPS and with the UPPS·TA complex was investigated by protein fluorescence spectroscopy. Our results suggested that tetramic acid binds to UPPS at an allosteric site adjacent to the FPP binding site. TA binds to free UPPS enzyme but not to substrate-bound UPPS. Unlike *Escherichia coli* UPPS which follows an ordered substrate binding mechanism, *Streptococcus pneumoniae* UPPS appears to follow a random-sequential substrate binding mechanism. Only one substrate, FPP or IPP, is able to bind to the UPPS·TA complex, but the quaternary complex, UPPS·TA·FPP·IPP, cannot be formed. We propose that binding of TA to UPPS significantly alters the conformation of UPPS needed for proper substrate binding. As the result, substrate turnover is prevented, leading to the inhibition of UPPS catalytic activity. These probe compounds and biophysical assays also allowed us to quickly study the mode of inhibition of other UPPS inhibitors identified from a high-throughput screening and inhibitors produced from a medicinal chemistry program.

Undecaprenyl pyrophosphate synthase (UPPS)[1] is an essential enzyme for bacterial viability. The C_{55} undecaprenyl pyrophosphate (UPP) produced by UPPS reaction is the lipid carrier for precursors of various cell wall structures, such as peptidoglycan, teichoic acids, and *O*-antigens (*1*). UPPS is highly conserved among Gram-positive and Gram-negative bacteria. The critical biological function of UPPS, as well as an active site amenable to small molecule inhibition as revealed by crystallographic structures (*2*−*5*), makes UPPS an attractive target for the discovery of novel antibacterial agents.

UPPS catalyzes the condensation of eight molecules of IPP with FPP (Scheme 1). Chen and co-workers examined the multiple-step kinetics of the UPPS reaction and defined the mechanism of the *Escherichia coli* UPPS reaction pathway using steady-state and pre-steady-state kinetic approaches (*6*). *E. coli* UPPS binds FPP and then IPP (ordered substrate binding mechanism). This initial substrate binding triggers eight continuous IPP condensation steps catalyzed by the enzyme leading to the final product C_{55}-UPP. Different product distributions were found with various enzyme:substrate and FPP:IPP ratios in the presence or absence of Triton. Triton is believed to activate UPPS activity by enhancing the rate of product dissociation and the rate of a protein conformational change (*6*).

UPPS inhibitors of the tetramic acid class have been identified by high-throughput screening (HTS) and a subsequent medicinal chemistry program (*7*). The complexity of the UPPS reaction mechanism makes the characterization of UPPS inhibitors using traditional enzyme kinetics rather challenging. To overcome this difficulty, we used biophysical approaches to investigate the mode of inhibition of this class of inhibitors. In this investigation, we applied an FPP fluorescent analogue (*8*) to evaluate the possibility of TA binding to the FPP binding site. A tetramic acid analogue containing a photosensitive moiety was used to probe the site of binding. The inhibition mechanism of tetramic acids was investigated by determining the interaction of a representative tetramic acid inhibitor with UPPS in the presence and absence of substrate analogues (*S*)-farnesyl thiopyrophosphate (FsPP) and (*S*)-isopentyl thiolopyrophosphate (IsPP) using photo-cross-linking and protein fluorescence spectroscopy. It was also shown that fluorescent probe displacement and competitive photo-cross-linking using the same photosensitive TA analogue can be used for quick identification of HTS hits that bind to the FPP or TA site.

MATERIALS AND METHODS

Reagent Supply. Substrates FPP (Figure 1A) and IPP were purchased from Sigma. FsPP (Figure 1B) and IsPP were purchased from Echelon Biosciences Inc. The fluorescent FPP analogue [Fluoro-probe (Figure 1C)] was chemically synthesized in house according to the published procedure (*8*). A photosensitive tetramic acid analogue [Photo-probe (Figure 1D)] was synthesized

*To whom correspondence should be addressed: 500 Technology Square, Cambridge, MA 02139. Telephone: (617) 871-7889. Fax: (617) 871-5791. E-mail: gejing.deng@novartis.com.

[1]Abbreviations: UPPS, undecaprenyl pyrophosphate synthase; IPP, isopentenyl pyrophosphate; FPP, farnesyl pyrophosphate; UPP, undecaprenyl pyrophosphate; TA, tetramic acid; FsPP, (*S*)-farnesyl thiopyrophosphate; IsPP, (*S*)-isopentyl thiolopyrophosphate; MOI, mode of inhibition; Tris, tris(hydroxymethyl)aminomethane; PBS, phosphate-buffered saline; HEPES, 4-(2-hydroxyethyl)-1-piperazineethanesulfonic acid; DMSO, dimethyl sulfoxide; HTS, high-throughput screening.

 Published on Web 05/17/2010

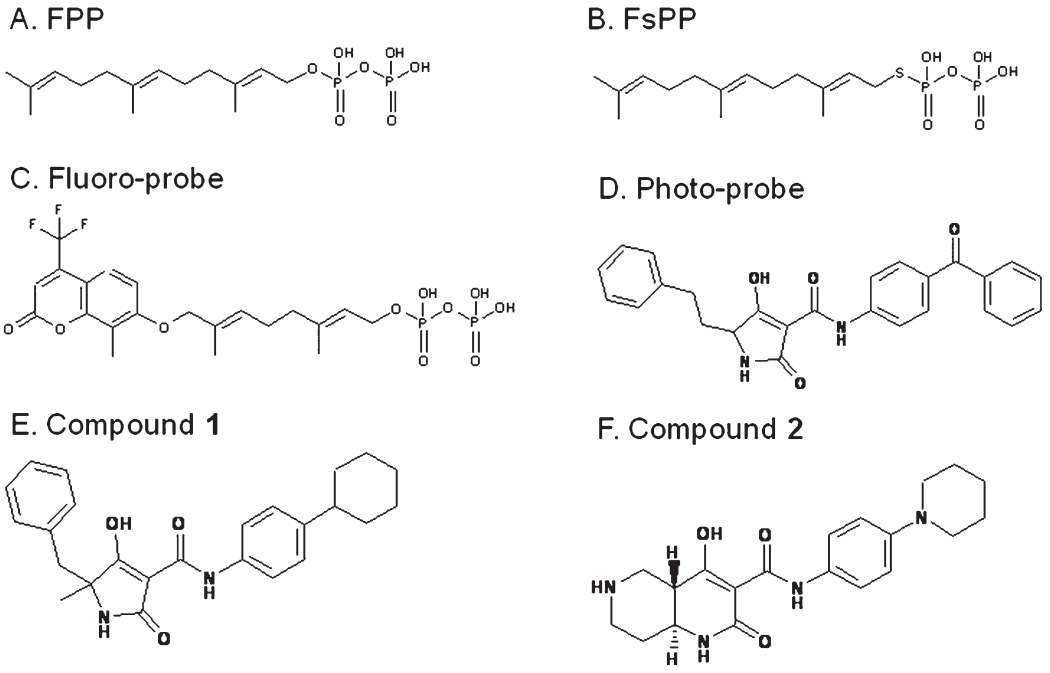

FIGURE 1: Chemical structures of compounds used in this study.

Scheme 1: Reaction Catalyzed by Undecaprenyl Pyrophosphate Synthase

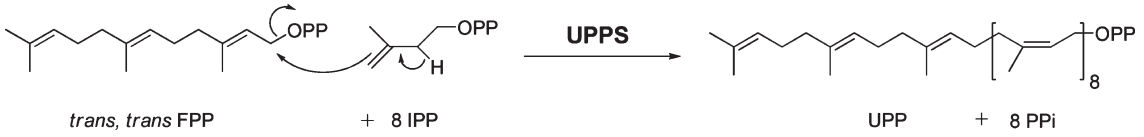

using the procedure described below. Compound **1** [5-benzyl-4-hydroxy-5-methyl-2-oxo-2,5-dihydro-1*H*-pyrrole-3-carboxylic acid (4-cyclohexylphenyl)amide, a representative tetramic acid (Figure 1E)] and compound **2** [(4a*S*,8a*S*)-4-hydroxy-2-oxo-1,2,4a,5,6,7,8,8a-octahydro[1,6]naphthyridine-3-carboxylic acid (4-piperidin-1-ylphenyl)amide, a representative non-tetramic acid (Figure 1F)] were also chemically synthesized (*9*, *10*). Total *E. coli* lipid extract was purchased from Avanti Polar Lipids, Inc. (Alabaster, AL). Biomol Green reagent was purchased from Enzo Life Sciences International, Inc. (formerly Biomol International, Inc.). 4-Aminobenzophenone, methyl malonyl chloride, and *N*-(4-aminophenyl)piperidine were purchased from Aldrich. 4-Cyclohexanylaniline was purchased from Lancaster Synthesis Inc. 2-Amino-2-methyl-3-phenylpropanoate was purchased from Chem-Impex International. Solvents and other reagents were purchased from Sigma-Aldrich or Fisher Scientific Inc. Water used in all experiments was HPLC-grade and was purchased from Sigma.

Expression and Purification of Streptococcus pneumoniae UPPS. The construct used for expression of *S. pneumoniae* UPPS was created using the pET15b expression vector consisting of a thrombin-cleavable N-terminal hexahistidine sequence followed by the *S. pneumoniae* UPPS sequence. pET15b-SpUPPS was transformed into competent *E. coli* BL21(DE3) Star host cells (Invitrogen), and they were grown at 37 °C on a culture plate containing imMedia AMP Agar (Invitrogen) until visible colonies were observed. Cells were transferred to a culture medium containing 5% EZ Mix Terrific Broth (Sigma), 1.5% (w/v) glucose, and 150 μg/mL ampicillin and grown at 37 °C to an OD_{600} of 2. Then 1 volume of sterilized glycerol was added to 4 volumes of the *E. coli* culture, which resulted in a high-density glycerol stock culture. Cells from the stock culture were transferred to a starter medium containing 5% EZ Mix Terrific Broth, 1 mM $MgSO_4$, 1.3% (w/v) glucose, and 150 μg/mL ampicillin and grown at 37 °C for 3 h. Following this, cells were diluted in fresh starter medium and grew at 30 °C overnight. Cells were harvested by centrifugation, and cell paste was suspended in sterilized Terrific Broth containing 1% glucose and 150 μg/mL ampicillin. Subsequently, the suspended cells was transferred into an "auto-induction" expression culture medium containing 1% (w/v) N-Z Amine AS (Sigma-Aldrich), 0.5% (w/v) yeast extract, 1 mM $MgSO_4$, 25 mM $(NH_4)_2SO_4$, 50 mM KH_2PO_4, 50 mM Na_2HPO_4, 0.5% (v/v) glycerol, 0.05% (w/v) glucose, 0.2% (w/v) α-lactose, and 150 μg/mL ampicillin and grown to an OD_{600} of 0.6. Cells were harvested via centrifugation and washed with a buffer containing 50 mM Tris (pH 7.5) and 100 mM NaCl. Cells were then resuspended, homogenized, lysed, and centrifuged. The supernatant was loaded onto a Ni-NTA column and washed with a buffer containing 50 mM HEPES (pH 7.3), 500 mM NaCl, 10% glycerol, 1 mM TCEP-HCl, EDTA-free protease inhibitor cocktail tablets (1 tablet/100 mL), and 20 mM imidazole and then washed with the same buffer containing 50 mM imidazole. His-tagged SpUPPS was eluted within a linear gradient from 200 to 300 mM imidazole. Fractions containing *S. pneumoniae* UPPS were pooled and subjected to centrifugal ultrafiltration against a buffer containing 50 mM HEPES (pH 7.3), 500 mM NaCl, 10% glycerol, 1 mM TCEP-HCl, and EDTA-free protease inhibitor cocktail tablets (1 tablet/100 mL). The protein was then loaded onto a Superdex-200PG HiLoad size-exclusion column (GE Healthcare) and eluted with a buffer containing 50 mM Tris (pH 7.5), 100 mM NaCl, and 10% glycerol. The identity of the purified protein was confirmed by mass spectrometry (measured molecular mass of 30735 Da, calculated molecular mass of 30737 Da with Met^1 cleaved). The purity of the protein was estimated to be 95% by SDS−PAGE.

Scheme 2: Synthesis of Photo-probe

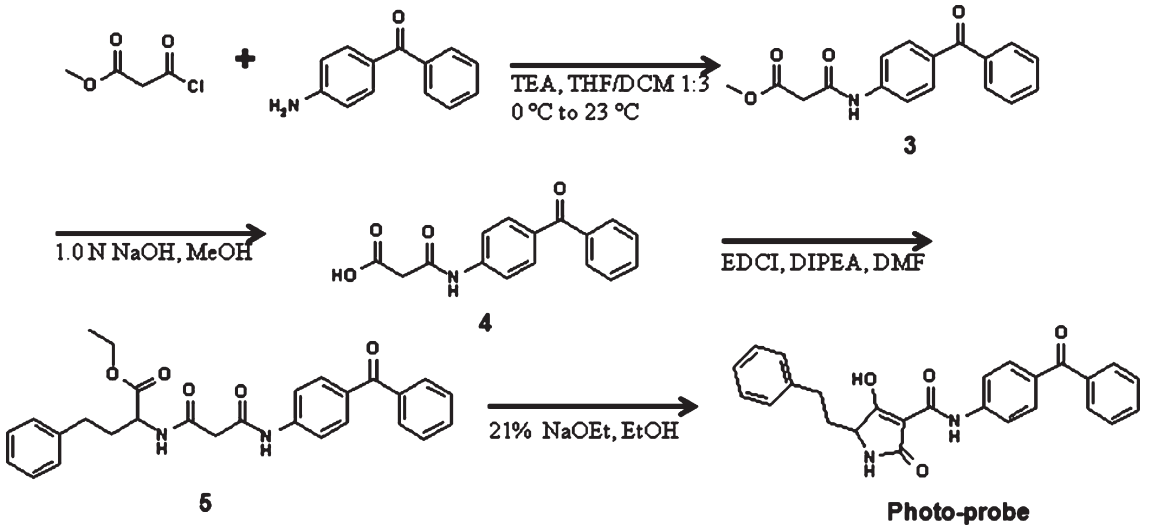

Synthesis of Photo-probe. Synthesis of Photo-probe was conducted using a four-step procedure starting from commercially available 4-aminobenzophenone and methyl malonyl chloride (Scheme 2) as described below.

Methyl 3-(4-Benzoylphenylamino)-3-oxopropanoate (*Compound **3***). To a well-stirred solution of 4-aminobenzophenone (3.95 g, 20 mmol) and triethylamine (5.5 mL, 40 mmol) in 20 mL of THF and 60 mL of dichloromethane (DCM) at 0 °C was added methyl malonyl chloride (2.73 g, 20 mmol) in 20 mL of DCM. The reaction mixture was stirred at 0 °C for 2 h and then stirred at room temperature for 16 h. The reaction was quenched with 50 mL of an aqueous solution of $NaHCO_3$. The organic phase was separated, and the aqueous layer was washed with 50 mL of DCM. The organic phases were combined, washed with brine, dried over $MgSO_4$, filtered, and concentrated in vacuum. The residue was purified by flash column chromatography on silica gel with an ethyl acetate/heptane mixture (10:90 to 30:70). This procedure produced 3.3 g of compound **3** (56% yield): ^{1}H NMR (400 MHz, DMSO-d_6) δ 11.58 (broad, 1H), 7.76−7.81 (m, 4H), 7.71−7.74 (m, 2H), 7.61−7.63 (m, 1H), 7.51−7.55 (m, 2H), 3.76 (s, 3H), 3.21 (bs, 2H); calculated molecular mass of $C_{17}H_{15}NO_4$, 297 Da; measured MS ES$^+$ m/z 298 and MS ES$^-$ m/z 296.

3-(4-Benzoylphenylamino)-3-oxopropanoic Acid (*Compound **4***). To a solution of methyl 3-(4-benzoylphenylamino)-3-oxopropanoate (3.2 g, 10.8 mmol) in 100 mL of methanol was added 1.0 N aqueous NaOH (32.4 mL, 32.4 mmol). The resulting mixture was stirred at room temperature for 16 h. Organic solvent was removed under reduced pressure, and the residue was cooled with an ice bath. A 1.0 N HCl solution was added to adjust the pH to < 5. The resulting solid was filtered and dried. The procedure produced 2.6 g of compound **4** (85% yield): ^{1}H NMR (400 MHz, DMSO-d_6) δ 11.58 (broad, 1H), 7.74 (s, 4H), 7.71 (m, 2H), 7.66 (m, 1H), 7.55 (m, 2H), 3.21 (s, 2H); calculated molecular mass of $C_{16}H_{13}NO_4$, 283 Da; measured MS ES$^+$ m/z 284, MS ES$^-$ m/z 282.

Ethyl 2-[3-(4-Benzoylphenylamino)-3-oxopropanamido]-4-phenylbutanoate (*Compound **5***). To a stirred mixture that contained 3-(4-benzoylphenylamino)-3-oxopropanoic acid (283 mg, 1.0 mmol), ethyl-2-homophenylalanine (243 mg, 1.0 mmol), diisopropylethylamine (DIPEA, 0.53 mL, 3.0 mmol), and dimethylformamide (DMF, 8 mL) was added 1-ethyl-3-(3-dimethylaminopropyl)carbodiimide (EDCI, 350 mg, 1.1 mmol). The mixture was stirred at room temperature for 16 h. The mixture was poured into 80 mL of an ice/water mixture and was extracted twice with 100 mL of ethyl acetate each time. The combined organic phase was washed with brine, dried over Na_2SO_4, filtered, and concentrated in vacuum. The residue was purified by flash column chromatography on silica gel with an ethyl acetate/heptane mixture (20:80 to 80:20) which resulted in 400 mg of compound **5** (85% yield): ^{1}H NMR (400 MHz, $CDCl_3$) δ 9.73 (s, 1H), 7.74−7.76 (d, 2H), 7.69−7.71 (m, 2H), 7.61−7.64 (d, 2H), 7.49−7.53 (m, 1H), 7.39−7.43 (m, 2H), 7.19−7.23 (m, 2H), 7.12−7.16 (d, 1H), 7.07−7.12 (m, 2H), 6.56−6.62 (d, 1H), 4.55−4.62 (m, 1H), 4.11−4.19 (q, 2H), 3.21−3.33 (dd, 2H), 2.58−2.66 (m, 2H), 2.15−2.25 (m, 1H), 1.98−2.08 (m, 1H), 1.21−1.26 (t, 3H); calculated molecular mass of $C_{28}H_{28}N_2O_5$, 472 Da; measured MS ES$^+$ m/z 473, MS ES$^-$ m/z 471.

N-(4-Benzoylphenyl)-4-hydroxy-2-oxo-5-phenethyl-2,5-dihydro-1H-pyrrole-3-carboxamide (*Photo-probe*). To a solution of compound **5** (400 mg, 0.85 mmol) in 10 mL of ethanol was added 21% NaOEt in ethanol (830 mg, 2.54 mmol). The mixture was stirred at room temperature for 24 h. Ethanol was removed by vacuum; 10 mL of an ice/water mixture was added, and the residue was acidified to pH < 5 with 1.0 N aqueous HCl. A solid was formed, filtered, and dried in vacuum. The procedure produced 340 mg of a white solid (94% yield): ^{1}H NMR (400 MHz, DMSO-d_6) δ 11.24 (broad, 1H), 7.70−7.75 (m, 5H), 7.67−7.69 (m, 2H), 7.62−7.66 (m, 1H), 7.53−7.57 (m, 3H), 7.27−7.30 (m, 2H), 7.21−7.23 (m, 2H), 7.15−7.20 (m, 1H), 3.60−3.67 (s, 1H), 2.62−2.68 (m, 2H), 1.96−2.02 (m, 1H), 1.63−1.69 (m, 1H); calculated molecular mass of $C_{26}H_{22}N_2O_4$, 426 Da; measured MS ES$^+$ m/z 427, MS ES$^-$ m/z 425.

Biomol Green Assay. UPPS activity was analyzed by a Biomol Green assay after the pyrophosphate generated by the UPPS reaction had been converted to inorganic phosphate by pyrophosphatase. The purified *S. pneumoniae* UPPS used in this assay was mixed with liposome made from total *E. coli* lipid extract in a 1:2 ratio (w/v). The enzyme reaction was conducted in 100 mM Tris-HCl (pH 7.3), 50 mM KCl, 1 mM $MgCl_2$, 0.01% Triton X-100, 20 μg/mL BSA, 3 μM FPP, 16 μM IPP, and 2 units/mL *E. coli* pyrophosphatase. The inorganic phosphate was then quantified with Biomol Green reagent according to the vendor's instructions.

Photo-Cross-Linking. Photo-cross-linking was performed using an RPR-100 Rayonet Photochemical Chamber Reactor

(Southern New England Ultra Violet Co.). UPPS (30 μM) was preincubated with 30 μM Photo-probe for 15 min at room temperature followed by UV exposure with the 350 nm lamps for 10−15 min. Dose-dependent competitive photo-cross-linking experiments were conducted using the same procedure except that unlabeled compound (0−200 μM) was included in the preincubation mixture. For studies involving prebound substrate, the substrate analogue was preincubated with UPPS for 10 min prior to addition of Photo-probe. Samples were prepared in 1× PBS (pH 7.4). The total volume of the sample mixture was 20 μL. To prevent self-cross-linking of UPPS induced by short UV light, the sample mixture of UPPS and Photo-probe were incubated in a borosilicate mass spectrometry (MS) sample tube. The MS sample tube was next lowered into a 15 mm × 160 mm borosilicate test tube and then placed in the carousel of the Rayonet Reactor for photo-cross-linking.

Mass Spectrometry. Intact protein mass spectrometry was conducted using an Agilent 1100 HPLC system interfaced with a Waters ZQ4000 single-quadrupole mass spectrometer with an electrospray ionization source operated in positive ion mode. Mass spectra were analyzed using MassLynx (Waters Inc.).

Peptide mapping was conducted using a capillary HPLC system (Agilent 1200) coupled to a QTrap4000 mass spectrometer (Applied Biosystems) operated in data-dependent mode. Protein was subjected to tryptic digestion after the protein had been denatured, reduced, and alkylated and extra alkylation reagent had been removed by dialysis. A Thermo LTQ ion trap mass spectrometer (Thermo Electron Corp.) was used to conduct MS^3 experiments.

Determination of the Equilibrium Binding Constant (K_D) of the Fluorescent Probe. The K_D of the fluorescent FPP analogue (named Fluoro-probe thereafter) for binding to *S. pneumoniae* UPPS was determined by titration of the UPPS enzyme (final concentrations of 0−15 μM) into a fixed amount of Fluoro-probe (final concentration of 2 μM) in a buffer containing 0.01% Triton X-100, 100 mM Tris-HCl (pH 7.5), 50 mM KCl, and 1 mM $MgCl_2$. The fluorescence intensity was measured with excitation at 336 nm and emission at 460 nm using a BMG PHERAstar Microplate Reader (BMG LABTECH GmbH). Data were fit using GraFit 5 to eq 1 (Morrison equation) (*11*) to produce the K_D value for Fluoro-probe binding.

$$F = \alpha I + (\beta - \alpha)\left\{\left[E + I + K_D^{probe} - \sqrt{(E+I+K_D^{probe})^2 - 4EI}\right]/2\right\} \quad (1)$$

where F is the measured fluorescence intensity, I is the concentration of Fluoro-probe, E is the concentration of UPPS, and α and β are scaling factors for low and high fluorescence intensities, respectively.

Fluorescent Probe Displacement. The fluorescent probe displacement assay was conducted at a fixed concentration of UPPS (3 μM) and fluorescent probe (2 μM), and varying inhibitor concentrations in a buffer containing 100 mM Tris-HCl (pH 7.5), 50 mM KCl, 1 mM $MgCl_2$, and 0.01% Triton X-100. Probe fluorescence increases with increasing concentrations of a competitive binder due to the displacement of Fluoro-probe from UPPS. Data were fit to eq 2 to yield an apparent K_D (K_D^{app}) value for inhibitor binding.

$$F = \alpha E + (\beta - \alpha)\left\{\left[E + I + K_D^{app} - \sqrt{(E+I+K_D^{app})^2 - 4EI}\right]/2\right\} \quad (2)$$

where I is the concentration of unlabeled inhibitor. Please note that in eq 2, the first term is αE instead of αI, as in eq 1.

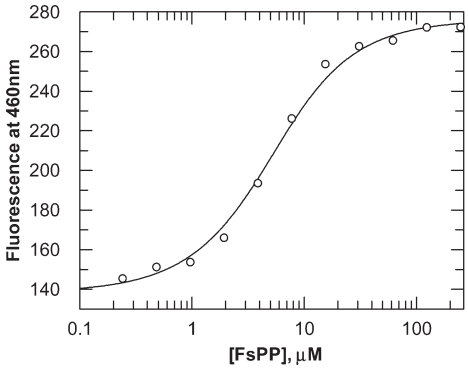

FIGURE 2: Competition of Fluoro-probe with FsPP for UPPS binding. Excitation at 336 nm and emission at 460 nm. The concentrations of Fluoro-probe and UPPS were fixed at 2 and 3 μM, respectively.

The true dissociation constant (K_D) of the UPPS·inhibitor complex was calculated using eq 3 [Cheng−Prusoff equation (*12*)].

$$K_D = \frac{K_D^{app}}{1 + \frac{[probe]}{K_D^{probe}}} \quad (3)$$

where K_D^{probe} and [probe] are the dissociation constant and concentration of Fluoro-probe, respectively.

The fluorescent probe displacement assay can also be conducted via titration of UPPS into a mixture of a fixed concentration of Fluoro-probe and testing compound. In the presence of a competitive binder, the apparent dissociation constant of the Fluoro-probe increases. The apparent dissociation constant of the UPPS·probe complex can be calculated using eq 1.

Fluorescence Binding Experiments. The protein fluorescence was determined using an Infinite M1000 microplate reader (Tecan Group Ltd.) or an RSM1000 spectrofluorometer (Olis, Inc.). Emission spectra were scanned in the range of 300−500 nm with an excitation wavelength of 285 nm. For studies involving prebound inhibitor, inhibitor was preincubated with UPPS for 15 min prior to addition of FsPP, IsPP, or both. All samples were prepared in buffer containing 100 mM HEPES (pH 7.3), 0.5 mM $MgCl_2$, 50 mM KCl, and 1.25% DMSO.

RESULTS

Fluorescent Probe Displacement. Chen and co-workers designed a fluorescent FPP analogue to study the interaction of the ligand with *E. coli* UPPS (*8*). We utilized this tool compound, i.e., Fluoro-probe, to study possible TA binding at the FPP binding site. This probe, when excited at its maximum absorbance wavelength (336 nm), emitted light at 460 nm linearly with the increase in probe concentration. Fluorescence self-quenching was not observed up to 10 μM probe (data not shown). Binding of the fluorescent probe to UPPS resulted in a decreased fluorescence intensity. This measurable change in intensity is the basis for the probe displacement assay (*8*). First, the dissociation constant of Fluoro-probe for binding to *S. pneumoniae* UPPS was determined via titration of UPPS into a fixed concentration of Fluoro-probe. Data were fit to eq 1 (ligand depletion considered) which resulted in a dissociation constant (K_D) of 0.25 μM.

The apparent dissociation constant of Fluoro-probe is expected to increase in the presence of increasing concentrations of competing inhibitors. To experimentally demonstrate this, we measured the fluorescence intensity of the probe at fixed concentrations of the probe and UPPS with varied concentrations

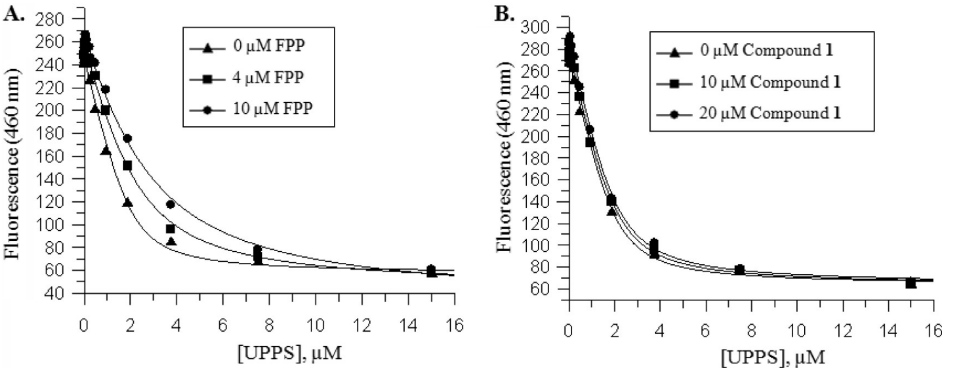

FIGURE 3: Identification of UPPS inhibitors that bind to the FPP binding site using Fluoro-probe. Excitation at 336 nm and emission at 460 nm. Each titration was performed via titration of UPPS into a fixed concentration of Fluoro-probe (2 μM) and compound (concentration indicated in the figure): (A) FPP and (B) compound **1**.

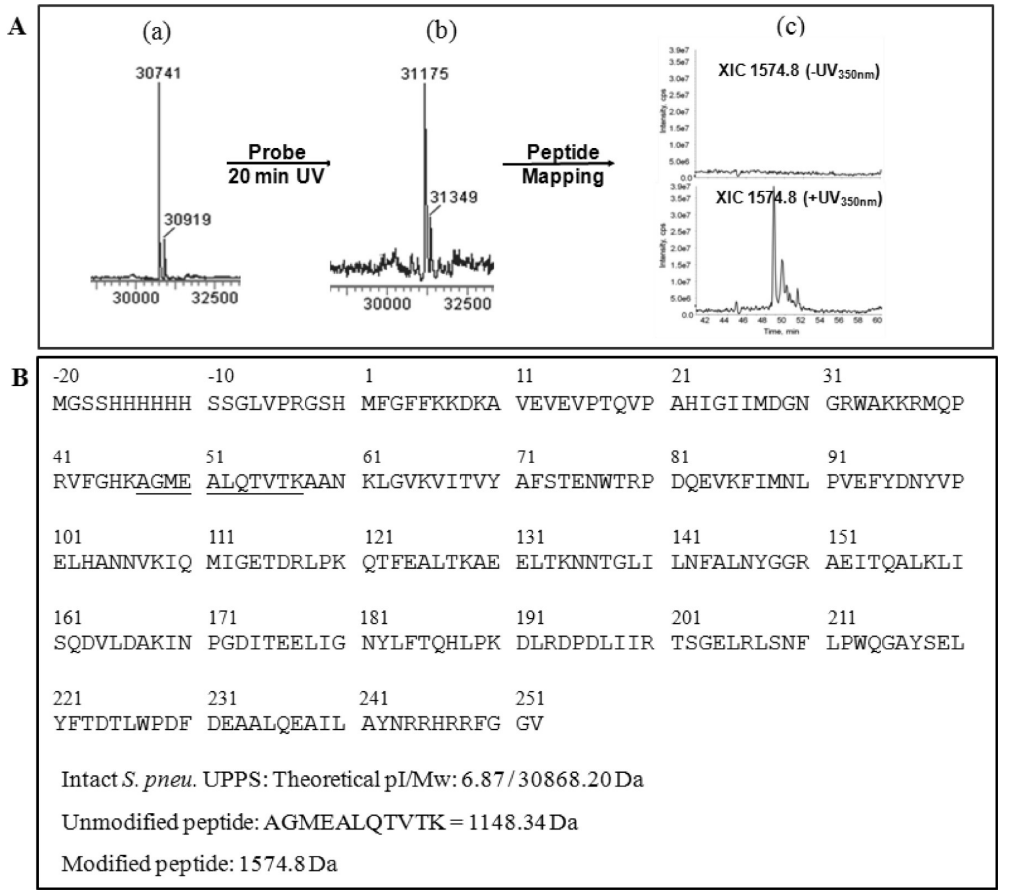

FIGURE 4: Identification of the peptide to which Photo-probe is covalently attached by mass spectrometry. (A) Mass spectra of intact UPPS before (a) and after (b) UV exposure (350 nm). The small peaks shown at 30919 Da in inset a and 31349 Da in inset b represent the small population of corresponding UPPS which contained a post-translational modification at its N-terminal His tag. The extracted ion chromatogram (XIC) of the modified peptide is shown in inset c. (B) Amino acid sequence of N-terminally His-tagged *S. pneumoniae* UPPS. The probe-modified peptide is underlined.

Scheme 3: Photo-Cross-Linking of a Compound That Contains a Benzophenone Moiety (circled) to a Protein (thick gray bar)

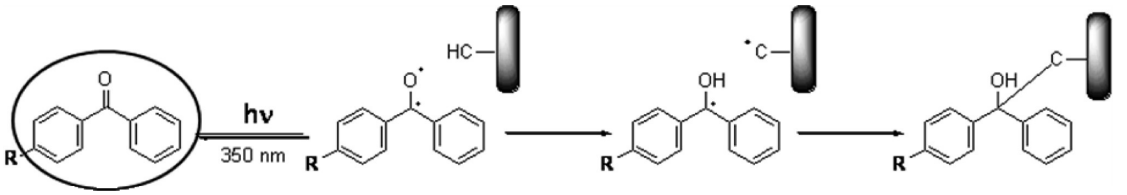

of FsPP. An increase in FsPP concentration resulted in the enhancement of the fluorescence of Fluoro-probe because of its displacement from UPPS by FsPP (Figure 2). Fitting the data to eq 2 resulted in an apparent K_D of 3.7 μM for FsPP binding. The true K_D value of FsPP is 0.41 μM as calculated using eq 3.

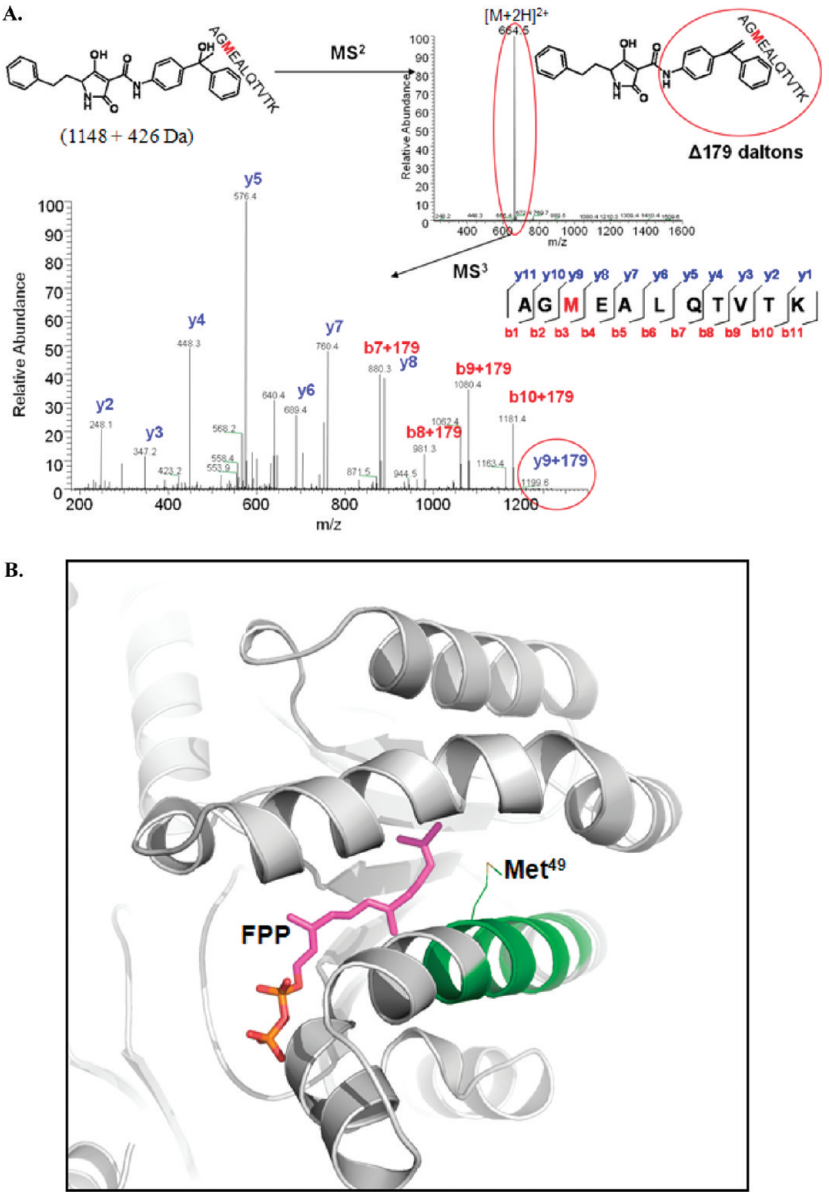

FIGURE 5: Identification of the site of Photo-probe attachment by tandem mass spectrometry. (A) MS^2 and MS^3 spectra. The Photo-probe-modified peptide (peptide + Photo-probe = 1148 Da + 426 Da = 1574 Da) was subjected to a low-energy fragmentation (MS^2). This fragmentation caused a bond cleavage within the Photo-probe structure, leaving part of the Photo-probe (179 Da) still attached to the peptide (red circle). The doubly charged ion of this fragment ($[M + 2H]^{2+}$ m/z 664.5) was subjected to a further fragmentation (MS^3). The resulting y and b ions (labeled in blue and red, respectively) revealed the peptide sequence as well as the site of Photo-probe attachment (red letter in the sequence). (B) X-ray structure of *S. pneumoniae* UPPS in complex with FPP (*5*) shown in cartoon representation. Protein is shown in ribbon and the substrate in sticks; part of helix α2 (AGMEALQTV) is colored green, of which the side chain of Met^{49} is shown.

Whereas the displacement of the probe can be measured at fixed concentrations of the probe and UPPS with varying competing compound concentrations, the reverse experiment could be conducted when the probe and competing compound concentrations were fixed and the UPPS concentration was varied. The advantage of the reverse titration is that any possible probe quenching by a competing compound can be factored in, because the interference is constant during UPPS titration. As an example, the competition between FPP and Fluoro-probe for UPPS is shown in Figure 3A. The apparent dissociation constant of Fluoro-probe changed from 0.26 μM at 0 μM FPP to 0.84 μM at 4 μM FPP and to 1.64 μM at 10 μM FPP.

Previous studies showed that Triton, a nonionic detergent, was essential for the in vitro enzymatic activity of UPPS, probably by mimicking the lipidic environment in which this enzyme may operate in vivo (*6*, *13*). Our study showed that ~25% of the fluorescence signal produced by 2 μM Fluoro-probe was quenched by 0.01% Triton and the signal completely quenched by 1% Triton. To balance between maintaining enzyme activity and obtaining robust fluorescence signals, we used 0.01% Triton X-100 for the fluorescent probe displacement assay. At this concentration, UPPS maintained ~70% activity (*14*).

The possibility of tetramic acid inhibitors binding to the FPP binding site was examined via titration of UPPS into a fixed concentration of Fluoro-probe and TA compound. The data showed that tetramic acids did not compete with Fluoro-probe, indicating that TA class inhibitors are not competitive inhibitors with respect to FPP. The result for a representative TA inhibitor, compound **1** (IC_{50} = 0.45 μM as determined by the Biomol Green assay), is shown in Figure 3B. Within experimental error, the dissociation constant of Fluoro-probe did not change with an increased concentration of compound **1**.

Identification of the TA Binding Site Using Photo-Cross-Linking and Mass Spectrometry. Benzophenone-based photolabeling has been extensively applied, especially for the determination of receptor−ligand binding sites (*15*). Upon light irradiation, a target specific compound containing a benzophenone photoreactive group can covalently attach to the protein to which it binds (Scheme 3).

We discovered that tetramic acids containing 1-phenylpiperidine or biphenyl groups showed enzyme inhibitory activity comparable to that of compound **1**. This led us to believe that a benzophenone substitution would create a photoreactive probe that binds and inhibits UPPS. A Photo-probe compound (Figure 1D) was designed and synthesized. It inhibited UPPS with an IC_{50} of 0.63 μM (as determined by the Biomol Green assay). Intact protein mass spectrometry showed that this probe compound (molecular mass of 426 Da) covalently modified UPPS with 1:1 molar ratio after the UPPS and Photo-probe mixture was exposed to long UV light in the 350 nm region (inset b in Figure 4A). As indicated in Materials and Methods, shielding by multiple layers of borosilicate glass was determined to be critical for the photo-cross-linking experiment as bleeding over of short UV light from the 350 nm lamps promoted self-cross-linking of two interacting UPPS monomers [UPPS forms a functional dimer in solution (*13*)]. Without borosilicate shielding, the covalent dimer was detected by SDS−PAGE after UV exposure (data not shown). This covalent dimer made mass spectrum deconvolution problematic.

Mass spectrometric analysis of UPPS alone indicated that the protein's N-terminal Met^1 was processed (calculated change in mass of −131 Da), and a small population of the protein contained a post-translational modification [the small peak with 178 Da of extra mass relative to UPPS (inset a in Figure 4A)]. This post-translational modification is likely due to a spontaneous α-*N*-6 gluconoylation often seen in His-tagged proteins (*16*). To identify the modification site of Photo-probe, the sample, after UV exposure, was subjected to trypsin digestion followed by peptide mapping using LC−MS. The analysis identified a peptide with a mass consistent with addition of Photo-probe [*m*/*z* 1574.8 (inset c in Figure 4A)]. The location of the peptide is underlined in the amino acid sequence of *S. pneumoniae* UPPS (Figure 4B).

The site of covalent attachment of Photo-probe was identified by tandem mass spectrometry. At a low collision energy, the amide bond present in the Photo-probe structure was cleaved while other amide bonds present in the peptide backbone remained intact. This resulted in a doubly charged fragment ion at *m*/*z* 664.5 (red circle in Figure 5A). This ion was subjected to further fragmentation (MS^3). This experiment not only confirmed the sequence of the probe-modified peptide but also revealed the site of probe attachment [Met^{49} (Figure 5A)]. According to the crystal structure of *S. pneumoniae* UPPS (*5*), Met^{49} is located in helix α2 close to the FPP binding site (Figure 5B). A systematic study of the photo-cross-linking of various amino acids with benzophenone showed that methionine is particularly favored in terms of reactivity and product stability (*17*). On the basis of this and the fluorescent probe displacement results, the binding site of TA appeared to be allosteric but adjacent to the FPP binding site.

Substrate Binding Order of S. pneumoniae UPPS. A fluorescence binding study conducted by Chen and colleagues showed that addition of FPP (or FsPP) to *E. coli* UPPS caused a reduction in the protein intrinsic fluorescence. In the presence of Mg^{2+}, the enhancement of fluorescence upon the binding of

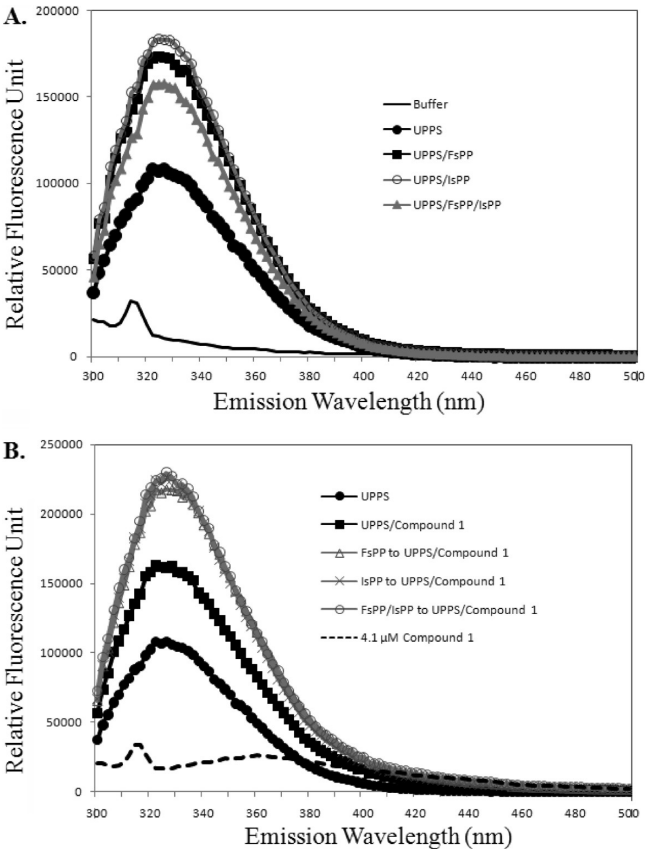

FIGURE 6: Fluorescence emission spectra of *S. pneumoniae* UPPS: (A) substrate binding to UPPS and (B) substrate binding to UPPS which was prebound with compound **1**. Final concentrations were as follows: 1 μM UPPS, 15 μM FsPP, 40 μM IsPP, and 5 μM compound **1**. Spectra are averages of two scans. Signals contributed by buffer blank and unbound compound **1** (4.1 μM, estimated on the basis of the IC_{50} value) have been subtracted.

IPP with the UPPS·FsPP complex was observed. The addition of IPP alone to UPPS failed to produce fluorescence change unless FPP (or FsPP) was preincubated with the enzyme (*18*). These data suggested that *E. coli* UPPS follows an ordered substrate binding mechanism. We conducted a similar substrate binding study with *S. pneumoniae* UPPS and found that in the presence of Mg^{2+} both FsPP (or FPP) and IsPP (or IPP) could bind and enhance the fluorescence of the enzyme in the absence of the other substrate (Figure 6A). This suggests that, unlike *E. coli* UPPS, *S. pneumoniae* UPPS likely follows a random-sequential substrate binding mechanism. Under the condition used, addition of both substrate analogues caused a reduction in fluorescence intensity relative to the fluorescence produced by the addition of one substrate (FPP or IPP) to UPPS (Figure 6A).

Inhibition Mechanism of Tetramic Acids. To study the inhibition mechanism of TA, the interactions of TA with various enzyme forms, including apo and substrate-bound *S. pneumoniae* UPPS, were investigated using the Photo-probe. Results showed that the probe molecule bound to and modified UPPS in the absence of substrate (Figure 7B) but did not do so when *S. pneumoniae* UPPS was prebound with either substrate analogue (Figure 7C,D). To investigate whether the formation of the UPPS·TA complex can prevent the substrate from binding, the interaction between substrate analogues and the UPPS·TA complex was examined using protein fluorescence spectroscopy. With excitation at 285 nm, the intrinsic fluorescence of *S. pneumoniae* UPPS increased upon addition of compound **1**,

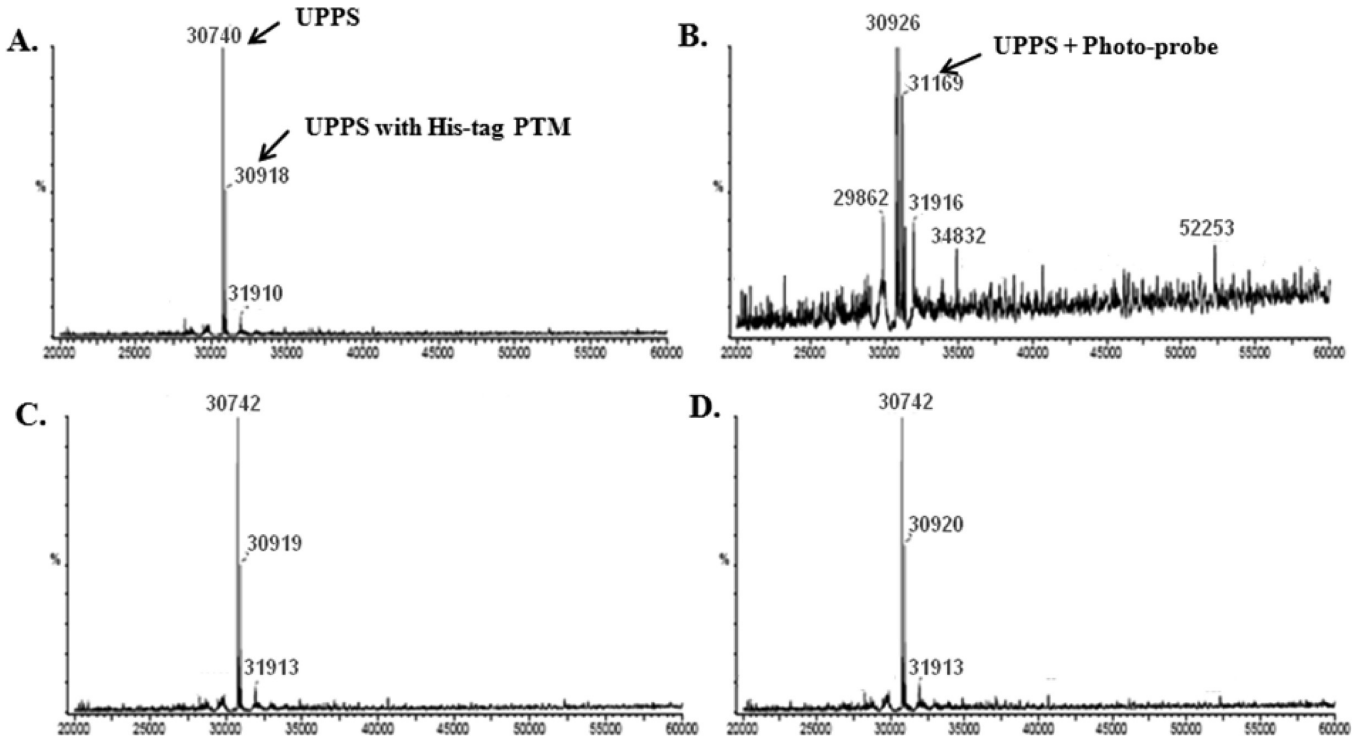

FIGURE 7: Interaction of tetramic acid with free or substrate-bound UPPS. Samples were analyzed by mass spectrometry after UV exposure (350 nm) at room temperature for 10 min: (A) 30 μM UPPS, (B) 30 μM UPPS and 30 μM Photo-probe, (C) 30 μM Photo-probe added to a preincubated mixture containing 30 μM UPPS and 100 μM FsPP, and (D) 30 μM Photo-probe added to a preincubated mixture containing 30 μM UPPS, 100 μM FsPP, and 100 μM IsPP. The small peak shown at ~30919 Da represents UPPS with a post-translational modification (PTM) at its N-terminal His tag.

indicating an interaction of tetramic acid with UPPS (Figure 6B). Addition of FsPP or IsPP to the preformed UPPS·TA complex caused a large increase of fluorescence relative to that of the UPPS·TA complex, suggesting the interaction of FsPP or IsPP with the UPPS·TA complex. Addition of IsPP to the preformed UPPS·TA·FsPP complex or addition of FsPP to the preformed UPPS·TA·IsPP complex did not produce a fluorescence change relative to the spectrum of the ternary complex, suggesting that the UPPS·TA·FsPP·IsPP quaternary complex was not formed (Figure 6B).

With excitation at 285 nm, compound **1** alone exhibited a low level of fluorescence at maximum emission ~40 nm above the maximum emission of UPPS (Figure 6B). To account for any fluorescence signal contributed by the unbound compound, the emission spectrum of compound **1** was subtracted from the emission spectra of UPPS samples containing compound **1**. The amount of unbound compound **1** in UPPS samples was estimated using the Morrison equation, assuming $K_D = IC_{50}$. The 20−22 nm blue shift observed in emission spectra obtained using an Infinite M1000 microplate reader (Tecan) compared to the emission spectra from the RSM1000 spectrofluorometer (Olis) is due to a light source intensity calibration engineered into the Infinite M1000 microplate reader. When uncalibrated data were retrieved by application of an instrument specific calibration file provided by Tecan, an emission spectrum similar to that obtained using RSM1000 was obtained (Figure S1 of the Supporting Information). With the microplate reader, we obtained very reproducible data. No photobleaching effect was observed.

Studying the Mode of Binding of New Compounds Using Fluoro-probe and Photo-probe. A number of HTS hits as well as compounds generated from a medicinal chemistry program were evaluated by performing fluorescent probe displacement using the Fluoro-probe and competitive photo-cross-linking using the Photo-probe. At a fixed concentration of Fluoro-probe, inhibitors that bind to the FPP binding site should compete with Fluoro-probe for binding to UPPS and show a competition profile similar to that illustrated in Figure 3A. Inhibitors that bind to the TA binding site should compete with Photo-probe for binding to UPPS, resulting in a reduced level of photo-cross-linking by the Photo-probe. As expected, compound **1** competed with Photo-probe for binding to UPPS in a dose response manner (Figure 8). To date, we have not identified a competitive inhibitor with respect to FPP. However, a bicyclic heterocycle compound (compound **2**) identified from a HTS follow-up effort was found to bind at the TA binding site (Figure S2 of the Supporting Information).

DISCUSSION

UPPS is an essential enzyme for bacterial viability and is highly conserved among Gram-positive and Gram-negative bacteria. The critical biological function of UPPS as well as an active site amenable to small molecule inhibition makes UPPS an attractive target for the discovery of novel antibacterial agents.

It has been demonstrated by HTS and a subsequent medicinal chemistry program that tetramic acids are potent and selective UPPS inhibitors (*7*). UPPS catalyzes the condensation of eight molecules of IPP with FPP. Depending on reaction conditions and the ratio of enzyme to substrate or ratio of FPP to IPP, reaction products of varying lengths can be generated (*6*). The dynamics of interactions of these products with UPPS has not been fully understood. The complexity of the reactions impedes the characterization of UPPS inhibitors by traditional enzyme kinetics. In this study, we used biophysical approaches to investigate the inhibition mechanism of TA class inhibitors.

Our data showed that TA did not compete with Fluoro-probe for binding to UPPS (Figure 3B), indicating that TA is not a competitive inhibitor with respect to FPP. The interactions between

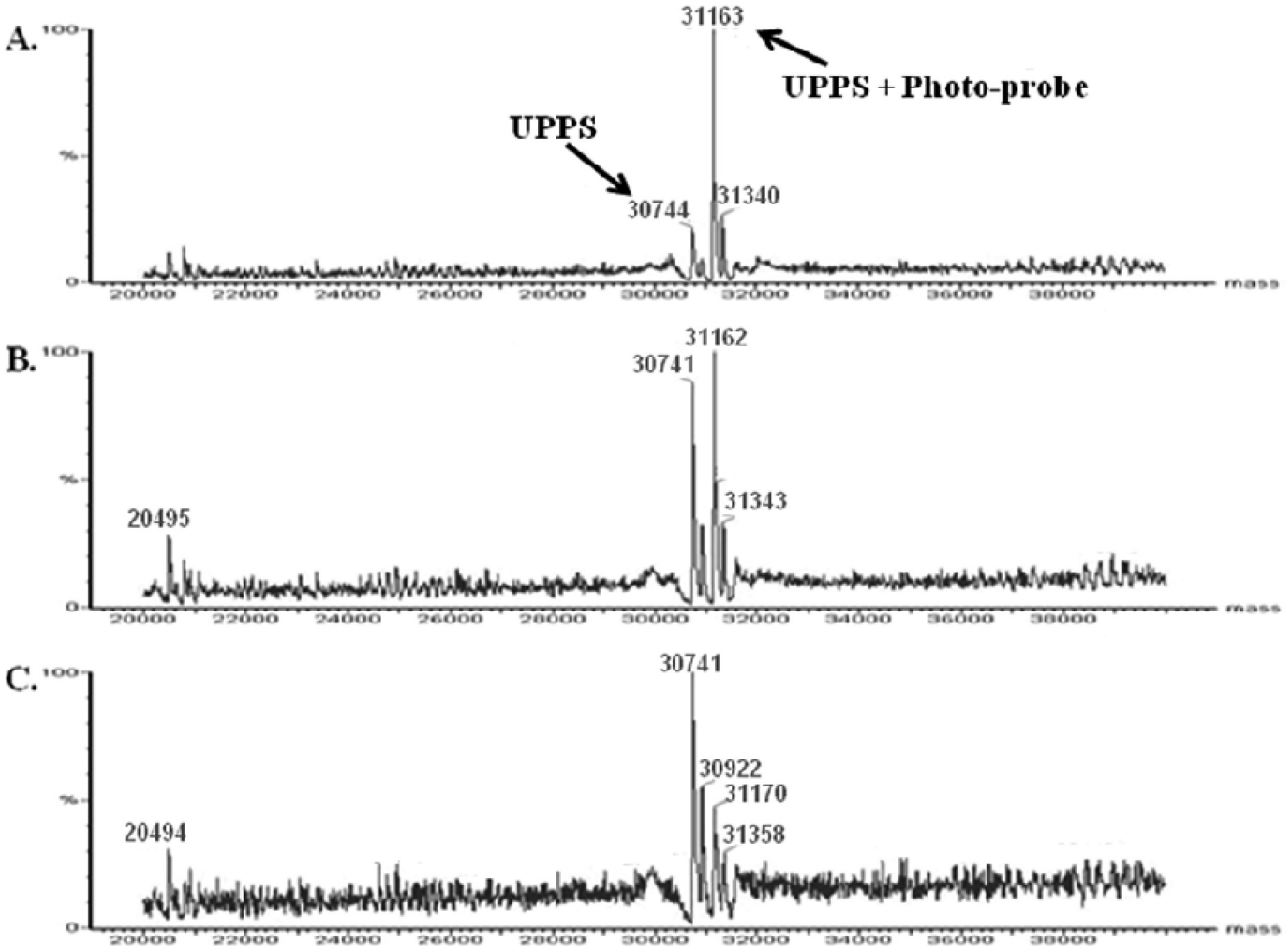

FIGURE 8: Compound **1** competes with Photo-probe for binding to UPPS in a dose response fashion. Samples were analyzed by mass spectrometry after UV exposure (350 nm) at room temperature for 15 min: (A) 30 μM UPPS and 30 μM Photo-probe, (B) 30 μM UPPS, 30 μM Photo-probe, and 100 μM compound **1**, and (C) 30 μM UPPS, 30 μM Photo-probe, and 200 μM compound **1**.

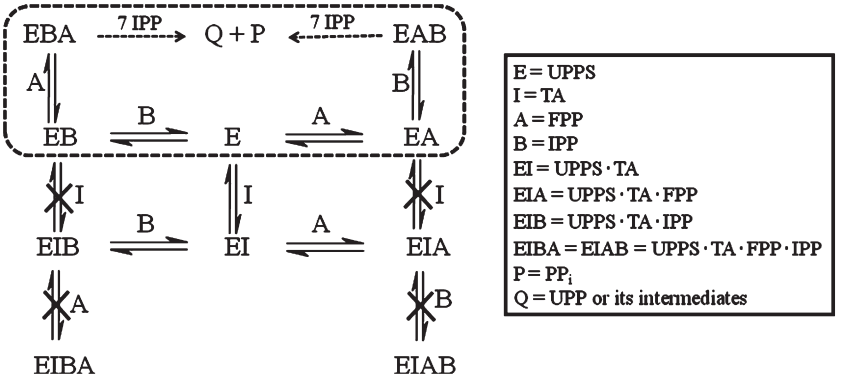

FIGURE 9: Proposed substrate binding mechanism of *S. pneumoniae* UPPS (dotted rectangle) and inhibition mechanism of tetramic acid. Dotted arrows represent the subsequent events after substrate binding needed for the first substrate turnover.

TA and various enzyme forms were investigated by photo-cross-linking and intact protein mass spectrometry. Our results indicated that the photosensitive TA analogue bound to and modified UPPS only when the enzyme was not prebound with substrates (Figure 7). Since the photo-cross-linking method monitors covalent modification of UPPS by Photo-probe, it cannot be used to study the interaction between the substrate and the preformed UPPS·TA complex. According to the crystal structure of *S. pneumoniae* UPPS (*5*), three tryptophan residues (W33, W77, and W227) are located near the substrate binding site and may be used to probe the interaction of the substrate with UPPS and with the preformed UPPS·TA complex. Unlike *E. coli* UPPS which follows an ordered substrate binding mechanism with FPP binding prior to IPP binding, our data for *S. pneumoniae* UPPS are consistent with a random-sequential substrate binding mechanism, with each substrate binding in a manner independent of the other (described by the dotted rectangle in Figure 9). TA enhanced the fluorescence of apo-UPPS, confirming the interaction between TA and

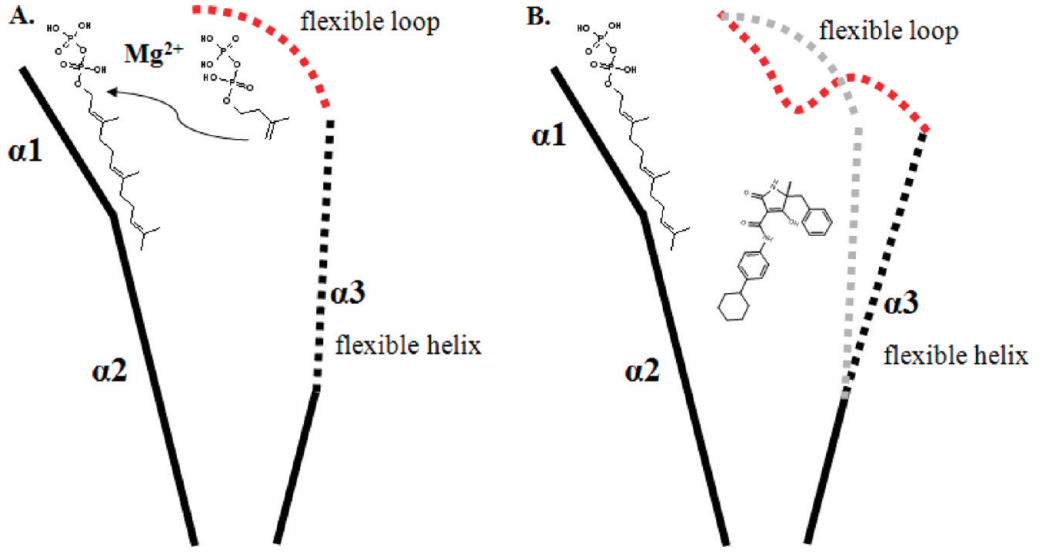

FIGURE 10: Proposed mode of binding of tetramic acid inhibitors: (A) substrate-bound UPPS and (B) the UPPS·TA·FPP ternary complex. The conformational change (red dotted line) upon binding of tetramic acid prevents IPP from binding to UPPS.

apo-UPPS. Addition of FsPP or IsPP to the preformed UPPS·TA complex caused a large enhancement in fluorescence relative to that of the UPPS·TA complex, suggesting that FPP or IPP can interact with the UPPS·TA complex and form the UPPS·TA·FsPP or UPPS·TA·IsPP complex. However, addition of the second substrate to the preformed UPPS·TA·FsPP or UPPS·TA·IsPP complex did not cause a fluorescence change relative to the spectra of the complexes (Figure 6B). This suggests that only one substrate can bind to the UPPS·TA complex but nonproductively. The contribution of each of the tryptophan residues in UPPS to the observed interactions remains unknown and needs to be further investigated.

The crystal structures of *S. pneumoniae* UPPS and *E. coli* UPPS are significantly structurally similar (*2*, *5*). Substrates FPP and IPP bind in an elongated hydrophobic tunnel surrounded by four β-strands (βA−βB−βD−βC) and two helices (α2 and α3). The lower part of the tunnel hosts the elongated reaction product as a result of consecutive condensation reactions. Our results showed that the Photo-probe bound and modified Met[49] in helix α2, suggesting that TA binds to an allosteric site adjacent to the FPP binding site in the elongated hydrophobic tunnel (Figures 5B and 10B). On the basis of the crystal structure of *E. coli* UPPS, the loop containing amino acids 72−82 (corresponding to amino acids 74−84 in *S. pneumoniae* UPPS), as illustrated by the red dots in Figure 10, was highly flexible and its electron density could not be seen in an apo-UPPS structure (*19*, *20*) but could be seen when Triton or FPP was bound (*3*, *4*). This loop is proposed to be associated with IPP binding and is responsible for bridging the interaction of IPP with FPP needed to initiate the condensation reaction and serving as a hinge to control the interchange between the closed (substrate-bound) protein conformation and the open (apoenzyme and product-bound) protein conformation (*18*, *19*). A large protein conformational change upon substrate binding was revealed using fluorescence quenching and stopped-flow methods (*18*). TA bound to apo-UPPS but not to the substrate-bound *S. pneumoniae* UPPS; we propose that this class of inhibitors binds to only the open conformation of *S. pneumoniae* UPPS. When UPPS is bound with substrates, the UPPS is locked to a closed conformation, preventing TA from entering the hydrophobic tunnel. TA did not compete with Fluoro-probe for binding and therefore is not a competitive inhibitor with respect to FPP. Since TA did not show binding to any preformed enzyme−substrate complex, it does not qualify to be, by definition, an uncompetitive or noncompetitive inhibitor. On the basis of the location of the Photo-probe attachment in the *S. pneumoniae* UPPS structure, TA likely binds to a deeper position in the hydrophobic tunnel relative to IPP. One substrate (FPP or IPP) can still bind to UPPS when it is bound with TA, but the second substrate cannot, suggesting that binding of TA to UPPS causes a conformational change that alters the substrate binding site, therefore preventing substrate turnover, leading to the inhibition of UPPS activity. On the basis of TA's binding site being distinct from the substrate binding site and its ability to alter enzyme activity, we classify TA into the allosteric inhibitor category. However, we do not know if UPPS activity is regulated by any allosteric mechanism related to the site where TA binds. On the basis of all the data presented above, we propose that TA inhibits UPPS by a mechanism as described in Figure 9. Further investigations are needed to confirm this mechanism.

To expand the use of these biophysical methods, we used Fluoro-probe and Photo-probe to determine the mode of inhibition of other interesting UPPS inhibitors identified from HTS as well as from a medicinal chemistry program. Inhibitors with the same binding mode as FPP and TA can be quickly identified by performing fluorescent probe displacement and competitive photo-cross-linking, respectively. As an example, compound **2** (a non-TA compound) was shown to bind at the TA binding site (Figure S2 of the Supporting Information).

Taken together, these biophysical approaches, including photo-cross-linking, fluorescent probe displacement, and protein fluorescence spectroscopy, have been successfully applied in studying the mode of binding and the inhibition mechanism of UPPS inhibitors identified from HTS. These tools are especially useful in cases where the cocrystal structures of UPPS and the inhibitor are not available.

ACKNOWLEDGMENT

We thank a few Novartis colleagues for their contributions to this work: Dr. James Koehn's lab for producing *S. pneumoniae* UPPS, Dr. Jovita Marcinkeviciene for critical review and helpful discussion of the manuscript, and Dr. Patricia Bradford for critical reading and editing of the manuscript.

SUPPORTING INFORMATION AVAILABLE

Comparison of emission spectra of *S. pneumoniae* UPPS scanned using a Tecan Infinite M1000 microplate reader and an Olis RSM1000 spectrophotometer and mass spectra showing competitive photo-cross-linking of Photo-probe with compound **2**. This material is available free of charge via the Internet at http://pubs.acs.org.

REFERENCES

1. Ogura, K., and Koyama, T. (1998) Enzymatic Aspects of Isoprenoid Chain Elongation. *Chem. Rev. 98*, 1263–1276.
2. Guo, R. T., Ko, T. P., Chen, A. P., Kuo, C. J., Wang, A. H., and Liang, P. H. (2005) Crystal structures of undecaprenyl pyrophosphate synthase in complex with magnesium, isopentenyl pyrophosphate, and farnesyl thiopyrophosphate: Roles of the metal ion and conserved residues in catalysis. *J. Biol. Chem. 280*, 20762–20774.
3. Chang, S. Y., Ko, T. P., Liang, P. H., and Wang, A. H. (2003) Catalytic mechanism revealed by the crystal structure of undecaprenyl pyrophosphate synthase in complex with sulfate, magnesium, and triton. *J. Biol. Chem. 278*, 29298–29307.
4. Chang, S. Y., Ko, T. P., Chen, A. P., Wang, A. H., and Liang, P. H. (2004) Substrate binding mode and reaction mechanism of undecaprenyl pyrophosphate synthase deduced from crystallographic studies. *Protein Sci. 13*, 971–978.
5. Concha, N. O., and Janson, C. A. (2003) Undecaprenyl pyrophosphate synthase (UPPS) enzyme and methods of use. WO 03/048733 A2.
6. Pan, J.-J., C, S.-T., and Liang, P.-H. (2000) Product distribution and pre-steady-state kinetic analysis of *Escherichia coli* undecaprenyl pyrophosphate synthase reaction. *Biochemistry 39*, 10936–10942.
7. Peukert, S., Sun, Y., Zhang, R., Hurley, B., Sabio, M., Shen, X., Gray, C., Dzink-Fox, J., Tao, J., Cebula, R., and Wattanasin, S. (2008) Design and structure-activity relationships of potent and selective inhibitors of undecaprenyl pyrophosphate synthase (UPPS): Tetramic, tetronic acids and dihydropyridin-2-ones. *Bioorg. Med. Chem. Lett. 18*, 1840–1844.
8. Chen, A. P., Chen, Y. H., Liu, H. P., Li, Y. C., Chen, C. T., and Liang, P. H. (2002) Synthesis and application of a fluorescent substrate analogue to study ligand interactions for undecaprenyl pyrophosphate synthase. *J. Am. Chem. Soc. 124*, 15217–15224.
9. Hurley, T. B., Lee, K., Peukert, S., and Wattanasin, S. (2008) Preparation of bicyclic heteroaryl amides as inhibitors of undecaprenyl pyrophosphate synthase. WO 2008014307.
10. Hurley, T. B., Peukert, S., and Wattanasin, S. (2008) Preparation of pyrrolecarboxamides and pyridinecarboxamides as inhibitors of undecaprenyl pyrophosphate synthase (UPPS). WO 2008014311.
11. Copeland, R. A. (2000) Protein-Ligand Binding Equilibria. In Enzymes. A Practical Introduction to Structure, Mechanism, and Data Analysis, 2nd ed., pp 76−108, Wiley-VCH, Inc., New York.
12. Cheng, Y., and Prusoff, W. H. (1973) Relationship between the inhibition constant (K1) and the concentration of inhibitor which causes 50% inhibition (I50) of an enzymatic reaction. *Biochem. Pharmacol. 22*, 3099–3108.
13. Allen, C. M. (1985) Purification and characterization of undecaprenylpyrophosphate synthetase. *Methods Enzymol. 110*, 281–299.
14. Li, H., Huang, J., Jiang, X., Seefeld, M., McQueney, M., and Macarron, R. (2003) The effect of triton concentration on the activity of undecaprenyl pyrophosphate synthase inhibitors. *J. Biomol. Screening 8*, 712–715.
15. Dorman, G., and Prestwich, G. D. (1994) Benzophenone photophores in biochemistry. *Biochemistry 33*, 5661–5673.
16. Geoghegan, K. F., Dixon, H. B., Rosner, P. J., Hoth, L. R., Lanzetti, A. J., Borzilleri, K. A., Marr, E. S., Pezzullo, L. H., Martin, L. B., LeMotte, P. K., McColl, A. S., Kamath, A. V., and Stroh, J. G. (1999) Spontaneous α-N-6-phosphogluconoylation of a "His tag" in *Escherichia coli*: The cause of extra mass of 258 or 178 Da in fusion proteins. *Anal. Biochem. 267*, 169–184.
17. Deseke, E., Nakatani, Y., and Ourisson, G. (1998) Intrinsic reactivities of amino acids towards photoalkylation with benzophenone: A study preliminary to photolabelling of the transmembrane protein glycophorin A. *Eur. J. Org. Chem. 1998*, 243–251.
18. Chen, Y. H., Chen, A. P., Chen, C. T., Wang, A. H., and Liang, P. H. (2002) Probing the conformational change of *Escherichia coli* undecaprenyl pyrophosphate synthase during catalysis using an inhibitor and tryptophan mutants. *J. Biol. Chem. 277*, 7369–7376.
19. Ko, T. P., Chen, Y. K., Robinson, H., Tsai, P. C., Gao, Y. G., Chen, A. P., Wang, A. H., and Liang, P. H. (2001) Mechanism of product chain length determination and the role of a flexible loop in *Escherichia coli* undecaprenyl-pyrophosphate synthase catalysis. *J. Biol. Chem. 276*, 47474–47482.
20. Fujihashi, M., Zhang, Y. W., Higuchi, Y., Li, X. Y., Koyama, T., and Miki, K. (2001) Crystal structure of cis-prenyl chain elongating enzyme, undecaprenyl diphosphate synthase. *Proc. Natl. Acad. Sci. U.S.A. 98*, 4337–4342.